

Calculation of Three-Dimensional Elastic Constants of Polymer Crystals. 2. Application to Orthorhombic Polyethylene and Poly(vinyl alcohol)

Kohji Tashiro, Masamichi Kobayashi, and Hiroyuki Tadokoro*

Department of Polymer Science, Faculty of Science, Osaka University, Toyonaka, Osaka 560, Japan. Received May 4, 1978

ABSTRACT: The theory of three-dimensional elastic constants described in the preceding paper has been applied to the typical crystalline polymers of different intermolecular interactions: orthorhombic polyethylene [van der Waals interaction] and poly(vinyl alcohol) [hydrogen bonding]. For orthorhombic polyethylene, the calculated anisotropic linear compressibilities and Young's moduli agree quite well with the experimental data. The atomic displacements and the potential energy distributions induced by tensile stress, hydrostatic pressure, and shearing stress have been illustrated. For poly(vinyl alcohol), the theoretical anisotropy of linear compressibilities and Young's moduli agree fairly well with the observed one. The role of hydrogen bonding on the crystallite modulus has been discussed.

In this paper, the method of calculation of three-dimensional elastic constants described in the previous paper¹ will be applied to the following two cases with different intermolecular interactions: (1) orthorhombic polyethylene (van der Waals interaction) and (2) poly(vinyl alcohol) (hydrogen bonding).

Orthorhombic polyethylene (PE) is a basically important substance in the field of structures and physical properties, and so becomes a starting point of discussion for other polymers. The elastic moduli along the longitudinal and transverse directions of PE were measured by Sakurada et al.² at room temperature. Ito et al.³ measured the linear and volume compressibilities of the PE crystal. The theoretical calculations of elastic constants of PE were made, based on the Born's lattice dynamical theory,⁴ by Odajima and Maeda,⁵ Wobser and Blasenbrey,⁶ and also Kitagawa and Miyazawa.⁷ Among these studies, the results calculated by Odajima and Maeda for the structure at 293 K are to be compared directly with the observed data, but the agreement between them seems not very good. Recently Kobayashi and Tadokoro⁸ proposed the pairwise intermolecular potential functions which reproduce the observed temperature dependence of vibrational frequencies, heat capacity, free energy, entropy, and so on of orthorhombic PE. Chatani et al.⁹ made the refinements of crystal structures of several kinds of PE sample by collecting the intensity data with enough accuracy using PSPC (position sensitive proportional counter). The authors will at first discuss the calculated results of elastic constants of the orthorhombic PE crystal, based on these potential functions and crystal structures.

As the second example, we deal with *atactic* poly(vinyl alcohol) (at-PVA). In the crystalline part of this polymer the molecules are linked together by intermolecular hydrogen bonding.^{10,11} The values of transverse crystallite moduli of at-PVA measured by Sakurada et al.² are larger than those of PE with only van der Waals interactions, indicating the large effect of hydrogen bonds. Quite recently, Ito et al.¹² have succeeded in measuring the anisotropic linear compressibilities of at-PVA by using the doubly oriented sample specimen. Thus we can compare the observed mechanical properties with the theoretical ones in detail from the viewpoint of the role of hydrogen bonding.

Results and Discussion

Orthorhombic Polyethylene. Crystal Structure and Potential Functions. In the previous paper,¹ the CH₂ unit was treated as a united atom. But we must separate C and H atoms individually in more strict dis-

Table I
Cell Constants and Setting Angles of
Orthorhombic Polyethylene

no.	a, Å	b, Å	c, Å	φ, ^a deg	ref
1	7.389	4.942	2.546	44.2 ^b	23
2	7.399	4.946	2.543	44.4	9
3	7.408	4.936	2.542	45.3	9
4	7.427	4.932	2.543	45.8	9
5	7.432	4.945	2.543	46.2	9
6	7.440	4.946	2.544	46.6	9
7	7.448	4.959	2.545	46.9	9
8	7.478	4.970	2.515	48.0	24

^a φ is the setting angle between the molecular plane and the bc plane. ^b Extrapolated value from the data of Chatani et al.⁹

cussion. The Young's modulus and linear compressibility change sensitively with the lattice parameters of samples prepared under various conditions: degree of crystallinity, branching, etc.^{2,3} Recently Chatani et al.⁹ clarified that the crystal structure of PE is affected by such factors as fine structure, branching, etc. Therefore in the calculation we employed the structural parameters refined by them for many kinds of sample of various sources (Table I). The positions of hydrogen atoms were determined by assuming ∠HCH = 109.5° and H-C = 1.09 Å. Intramolecular potentials are valence force field type, and the pairwise intermolecular ones are Buckingham type

$$V(r) = B \exp(-Cr) - Ar^{-6} \quad (1)$$

where *r* is an interatomic distance and *A*, *B*, and *C* are parameters. The intermolecular force constants were obtained as the second derivatives of these potential functions. All the H...H and C...H atomic pairs with interatomic distance shorter than 4 Å were taken into consideration. The C...C interactions were ignored since there are no C...C atomic pairs with *r* < 4 Å. The intramolecular potentials and the parameters *A*, *B*, and *C* are those that Kobayashi and Tadokoro⁸ have already proposed. These parameters can reproduce the temperature dependence of vibrational frequencies, heat capacities, and thermodynamical functions such as entropy. Besides, the cell parameters at the energy minimum at 10 K agree well with the observed ones.

The elastic and compliance constants, calculated with these potential and structural parameters, are shown in eq 2 and 3 for structure no. 2 in Table I, where 10¹⁰ dyn/cm² = 1 GPa.

A. Anisotropy of Young's Modulus and Linear Compressibility. Figure 1 shows the anisotropy of

$$C = \begin{bmatrix} 7.99 & 3.28 & 1.13 & 0 & 0 & 0 \\ 3.28 & 9.92 & 2.14 & 0 & 0 & 0 \\ 1.13 & 2.14 & 315.92 & 0 & 0 & 0 \\ 0 & 0 & 0 & 3.19 & 1.62 & 3.62 \\ 0 & 0 & 0 & 1.62 & 3.62 & 3.62 \\ 0 & 0 & 0 & 3.62 & 3.62 & 3.62 \end{bmatrix} \times 10^{10} \text{ dyn/cm}^2 \quad (2)$$

$$S = \begin{bmatrix} 14.48 & -4.78 & -0.02 & 0 & 0 & 0 \\ -4.78 & 11.67 & -0.06 & 0 & 0 & 0 \\ -0.02 & -0.06 & 0.32 & 0 & 0 & 0 \\ 0 & 0 & 0 & 31.31 & 61.86 & 27.60 \\ 0 & 0 & 0 & 61.86 & 27.60 & 27.60 \\ 0 & 0 & 0 & 27.60 & 27.60 & 27.60 \end{bmatrix} \times 10^{-12} \text{ cm}^2/\text{dyn} \quad (3)$$

Young's modulus in the ab plane. Young's modulus $E(\theta)$ in the direction of an angle θ from the a axis is represented as follows in the case of the orthorhombic system.¹³

$$1/E(\theta) = s_{11} \cos^4 \theta + s_{22} \sin^4 \theta + (2s_{12} + s_{66}) \sin^2 \theta \cos^2 \theta \quad (4)$$

The thick solid curve represents a curve fitted to the values observed by Sakurada et al.² for the (200), (020), and (110) planes. Bars in the radial directions indicate errors in measurements. The theoretical value (thin solid curve) is in the same order as the observed one, although the former is, strictly speaking, somewhat larger than the latter. The theoretical curve is slightly anisotropic and the Young's modulus in the b direction is larger than that in the a direction, contrary to the almost isotropic curve of observed values.

In Figure 2 the anisotropy of linear compressibility in the ab plane is shown. The linear compressibility $\beta(\theta)$ is expressed as¹³

$$\beta(\theta) = (s_{11} + s_{12} + s_{13}) \cos^2 \theta + (s_{21} + s_{22} + s_{23}) \sin^2 \theta \quad (5)$$

The thick solid line represents a curve fitted to the values observed by Ito et al.³ for the (200), (020), and (110) planes. Bars in the radial directions indicate errors in measurements. The agreement between the calculated (thin solid curve) and experimental results is quite good, although these results were obtained by quite different methods from each other. The values of linear compressibilities are obtained directly from the measured changes in the lattice spacing in variation with hydrostatic pressure. It is not necessary to make any assumption on the morphological model for the partially crystalline system, contrary to the series model for the case of elastic moduli. Therefore the agreement between observed and calculated values of linear compressibility indicate, conversely speaking, that the potentials used in calculation are considered to be reasonable. The measurement of Young's modulus in the directions perpendicular to the fiber axis is very difficult because the samples break easily. It should be noted here that Young's moduli cannot be derived from the observed values of linear compressibilities although the measurement of the latter is highly accurate as stated above.

The broken lines in Figures 1 and 2 represent respectively the theoretical curves of Young's modulus and linear compressibility at room temperature, obtained by Odajima and Maeda.⁵ The intermolecular force constants used by them are not so different from ours. The discrepancy in the resultant curve between two cases may be due to the difference in the setting angle assumed (they used the value of 42° instead of the present value of 44.4° from the b axis). It is much more important to use the setting angle

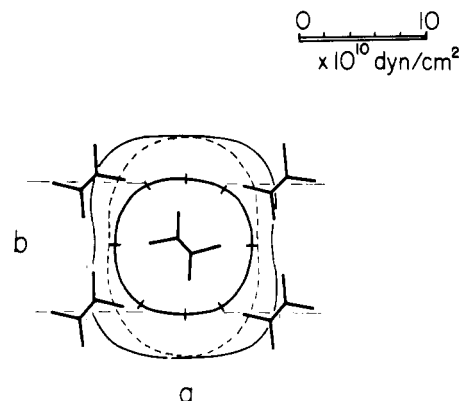


Figure 1. Anisotropy of Young's modulus in the ab plane of orthorhombic polyethylene: —, observed by Sakurada et al.² (293 K); —, calculated by the authors (293 K); ---, calculated by Odajima and Maeda⁵ (293 K).

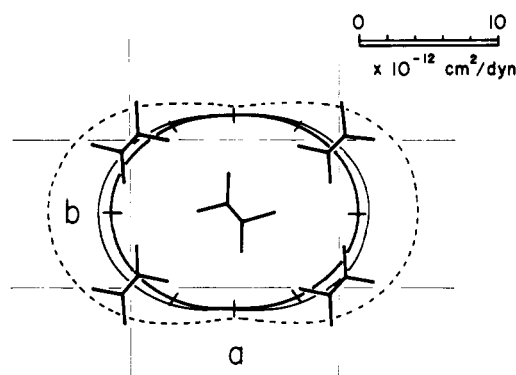


Figure 2. Anisotropy of linear compressibility in the ab plane of orthorhombic polyethylene: —, observed by Ito et al.³ (293 K); —, calculated by the authors (293 K); ---, calculated by Odajima and Maeda⁵ (293 K).

Table II
Observed Crystallite Modulus along the c Axis of Orthorhombic Polyethylene

method	value
X-ray diffraction ²	$235 \times 10^{10} \text{ dyn/cm}^2$
Raman spectroscopy ¹⁴	358 ± 25
Raman spectroscopy ^{a, 15}	290
neutron scattering ¹⁶	329

^a Value corrected by taking the interlamellar interactions into consideration.

obtained by the detailed analysis of crystal structure, as stated above.

In any way, however, the PE crystal may be deformed more easily into the direction of the a axis than the b axis.

B. Young's Modulus and Linear Compressibility along the c Axis. The Young's modulus along the c axis is calculated to be

$$E_c = 1/s_{33} = 315.5 \times 10^{10} \text{ dyn/cm}^2 \quad (6)$$

As shown in Table II, the observed values by various methods may be consistent with the calculated value. There exists, however, an appreciable discrepancy between the Young's moduli observed by inelastic neutron scattering¹⁶ and Raman spectroscopic¹⁴ (longitudinal acoustic mode or accordion-like mode) methods and that observed by the X-ray diffraction method.² The calculated value is closer to the former one. The calculated dispersion curves of the skeletal vibrations of PE agree well with those measured by the neutron scattering method.¹⁶ These circumstances suggest that we may properly compare the theoretical results with those obtained by neutron scat-

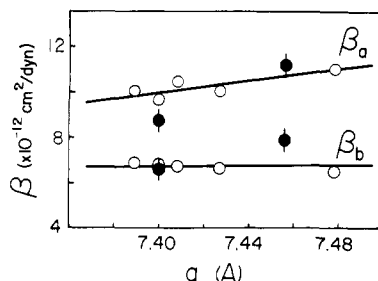
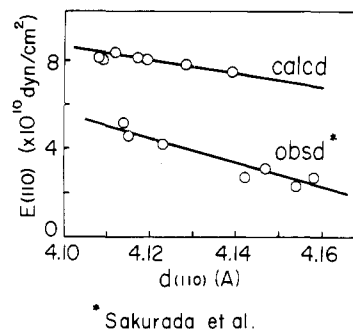


Figure 3. Dependence of linear compressibilities along the *a* and *b* axes on the *a* dimension: ●, the observed value by Ito et al.,³ and ○, the calculated value.



* Sakurada et al.

Figure 4. Dependence of Young's modulus along the (110) direction on the lattice spacing *d*(110). Observed values are after Sakurada et al.²

tering measurements. One method of filling up a gap between dynamical and static methods would be the reinterpretation of observed Raman and neutron scattering data by introducing the intermolecular interaction, as Strobl and Eckel have done.¹⁵ But the magnitude of this interaction is at most 10×10^{10} dyn/cm², which does not have a large enough effect to stop a gap between two kinds of methods. This will be an important problem to study in the future.

The calculated value of linear compressibility along the *c* axis is 0.235×10^{-12} cm²/dyn, while the observed one is

about 0.13×10^{-12} cm²/dyn by Ito et al.³ The measured datum is only one, as they said, and therefore the more detailed measurement will be desirable.

C. Poisson's Ratio and Volume Compressibility.

Poisson's ratios of the *a* and *b* axes to a tensile stress along the *c* axis are given by¹⁷

$$\nu_{i3} = -s_{i3}E_c \quad (7)$$

where *i* = 1 and 2. The theoretical values are $\nu_{13} = 0.06$ and $\nu_{23} = 0.20$, and their average is 0.13, which are a little smaller than the value 0.3 assumed for the ordinary low molecular weight single crystals.³

Volume compressibility κ is given as follows.¹³

$$\kappa = s_{11} + s_{22} + s_{33} + 2(s_{12} + s_{23} + s_{13}) \quad (8)$$

The calculated value $\kappa = 16.75 \times 10^{-12}$ cm²/dyn is in good agreement with the observed value 15.4×10^{-12} cm²/dyn by Ito et al.³

D. Changes of Linear Compressibilities and Young's Moduli. As stated earlier, the linear compressibilities and Young's moduli vary appreciably with the changes of cell constants or lattice strains of samples.^{2,3} As shown in Figures 3 and 4, linear compressibilities increase and Young's moduli decrease gradually with the increment of lattice spacings of the *a* axis or (110) plane, respectively. The linear compressibilities along the *a* and *b* axes and the Young's modulus in the direction normal to the (110) plane are calculated by using the lattice constants and setting angles of PE crystals listed in Table I. Figures 3 and 4 compare the calculated and observed values. The changes of linear compressibility with the length of the *a* axis agree fairly well with the observed ones.³ The theoretical changes of Young's modulus may also be consistent with the observed ones,² although the absolute values are as a whole larger than the observed ones as stated above.

E. Atomic Displacements and Potential Energy Distributions. In the previous papers,^{18,19} we introduced a new idea of potential energy distributions, that is, the distributions of strain energy to the internal coordinates when the crystal is deformed. Figure 5 shows the energy

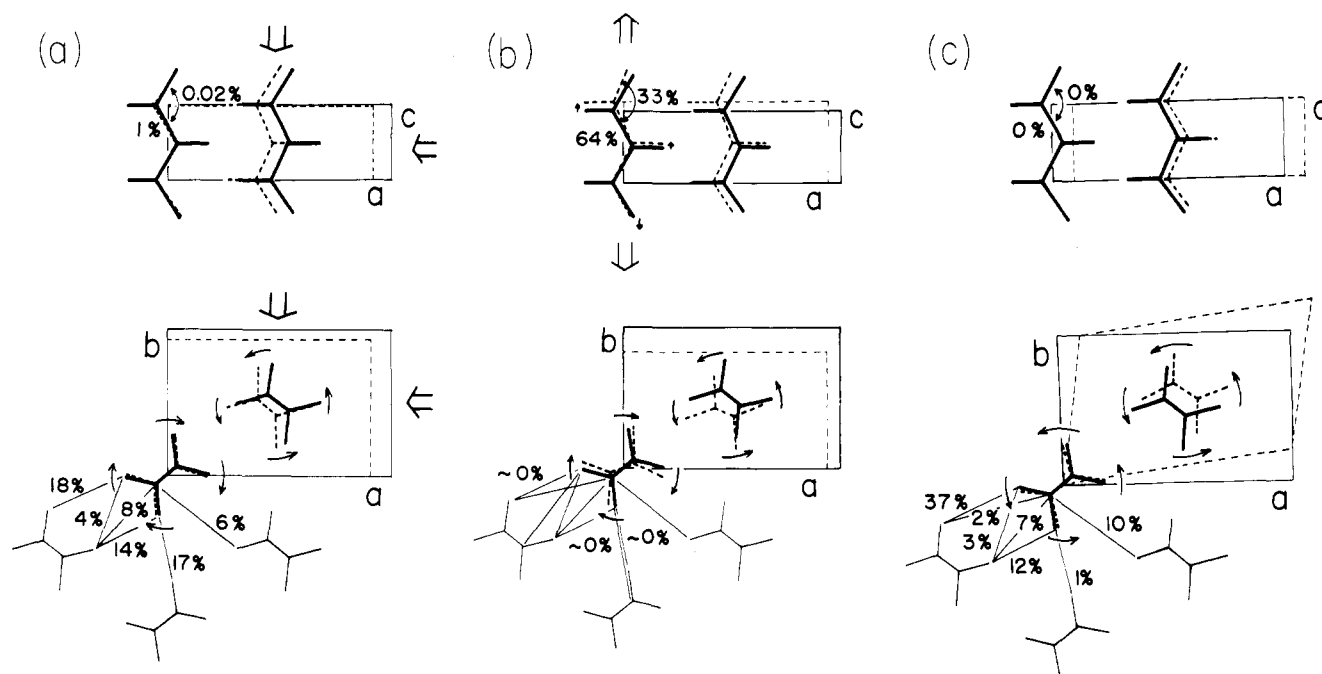


Figure 5. Atomic displacements and potential energy distributions when the orthorhombic polyethylene crystal is deformed by (a) hydrostatic pressure of 10 kbar, (b) tensile stress of 30×10^{10} dyn/cm² along the chain axis, and (c) shear stress of 1×10^{10} dyn/cm² in the *ab* plane.

distributions and atomic displacements when the PE crystal responds under stress in the various directions: the cases of (a) hydrostatic pressure, (b) the tensile stress along the c axis, and (c) the shear stress in the ab plane (for structure no. 2 in Table I).

As shown in Figure 5a and 5b, the molecular chains tend to rotate around the c axis so as to increase the value of the setting angle (from the b axis), by the tensile stress along the chain axis and also by the hydrostatic pressure from all directions. The latter case, especially, corresponds well to the results of lattice energy calculations reported by Seto et al.²⁰ that the setting angle giving the energy minimum becomes larger with the increment of pressure. The strain energy produced by hydrostatic pressure is concentrated to the changes of intermolecular nonbonded-interatomic distances, especially the H...H atomic pairs. The molecular chains are hardly deformed, meaning the great stiffness of chains against the compression along the chain axis, i.e., the linear compressibility along this direction is quite small. On the other hand, in the case of tensile stress, about 97% of the strain energy is distributed to the deformation of molecular chains and the potential energy distributions to the intermolecular atomic pairs are quite small ($\leq 0.005\%$), in contrast to the case of hydrostatic pressure. Nevertheless the molecular plane tends to incline toward the a axis by the tensile stress along the c axis. That is to say, the changes of setting angle are made by the slight energy of strain. Therefore such rotations of chains may be one of the factors governing the difference in setting angle among the various PE samples of different history (Table I); for example, the so-called "residual stress" remaining inside the PE samples prepared by various methods may influence the setting angle of the chains.

Poly(vinyl alcohol). Crystal Model and Potential Functions. As found in the previous section for orthorhombic PE, the propriety of potential functions and structure model is essential to the calculation of crystallite modulus. For poly(vinyl alcohol), we used here the crystal structure first proposed by Bunn¹⁰ and refined by Nitta et al.¹¹ except for assuming the molecular chains of *syn-diotactic* configuration instead of *atactic* configuration. The potential functions were directly transferred from the results of normal coordinate treatments of the PVA crystal using the polarized infrared (including far infrared) and Raman spectra of doubly oriented PVA samples.²¹ The spectroscopic studies will be reported elsewhere.²¹

A. Anisotropy of Linear Compressibility. The calculated elastic and compliance constants are given in eq 9 and 10 where the rectangular coordinate axes are

$$C = \begin{bmatrix} 21.79 & 7.72 & 2.98 & 0 & 0 & 3.76 \\ 7.72 & 11.95 & 3.30 & 0 & 0 & 1.08 \\ 2.98 & 3.30 & 288.47 & 0 & 0 & -0.29 \\ 0 & 0 & 0 & 10.78 & 0.12 & 0 \\ 0 & 0 & 0 & 0.12 & 1.64 & 0 \\ 3.76 & 1.08 & -0.29 & 0 & 0 & 4.28 \end{bmatrix} \times 10^{10} \text{ dyn/cm}^2 \quad (9)$$

$$S = \begin{bmatrix} 6.87 & -3.98 & -0.03 & 0 & 0 & -5.04 \\ -3.98 & 10.90 & -0.08 & 0 & 0 & 0.73 \\ -0.03 & -0.08 & 0.35 & 0 & 0 & 0.07 \\ 0 & 0 & 0 & 9.28 & -0.68 & 0 \\ 0 & 0 & 0 & -0.68 & 61.05 & 0 \\ -5.04 & 0.73 & 0.07 & 0 & 0 & 27.59 \end{bmatrix} \times 10^{-12} \text{ cm}^2/\text{dyn} \quad (10)$$

assumed as z = chain axis (b), y = c axis, and x normal to the zy plane.

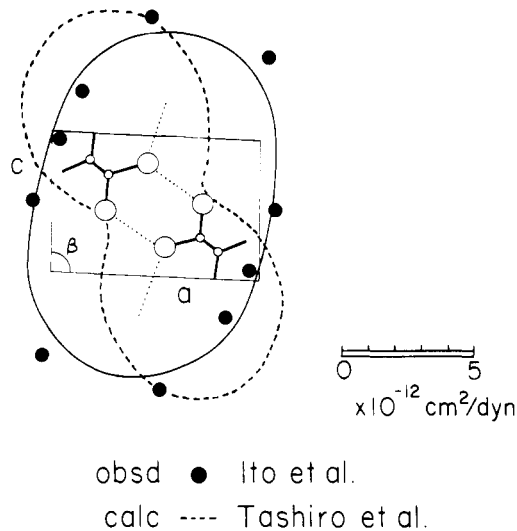


Figure 6. Anisotropy of linear compressibility in the ac plane of poly(vinyl alcohol): —, observed by Ito et al.¹²; ---, calculated by the authors.

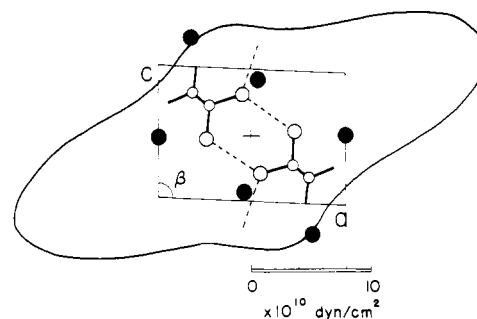


Figure 7. Anisotropy of Young's modulus in the ac plane of poly(vinyl alcohol). ● represents the observed value by Sakurada et al.²

Recently Ito et al.¹² have measured the anisotropy of linear compressibility of the at-PVA crystal by using doubly-oriented sample. The solid line in Figure 6 shows the curve which was obtained by the least-squares treatment of their observed data (solid circles). The broken line represents our calculated result. The relative sizes of calculated linear compressibilities along the a and c axes agree fairly well with the observed ones. However, strictly speaking, the maximal direction of the observed anisotropic curve deviates about 30° from the theoretical one. The anisotropy of the mechanical properties may be affected by the disorder in the crystal structure and so on. The reason for the above discrepancy will be a future problem.

Volume compressibility is calculated to be

$$\kappa = 9.94 \times 10^{-12} \text{ cm}^2/\text{dyn}$$

in good agreement with the observed value of about $11 \times 10^{-12} \text{ cm}^2/\text{dyn}$.¹² Different from the case of anisotropy of linear compressibility, volume compressibility is approximately given as follows,

$$\kappa \approx 1/V(\partial^2 U_0/\partial V^2) \quad (11)$$

where U_0 is the lattice energy and V the volume of the unit cell.³ That is to say, the volume compressibility is mainly determined by the density or the packing coefficient of the unit cell, not by the "direction" of intermolecular atomic pairs which will influence the anisotropy of linear compressibility.

B. Anisotropy of Young's Modulus. In Figure 7 is shown the anisotropy of Young's modulus in the ac plane

perpendicular to the chain axis. The solid circles in the figure represent the observed values by Sakurada et al.² The solid curve is our calculated result. The magnitudes of the observed and calculated results are in the same order, except for the direction of the maximal value of the calculated anisotropy for which the observed value is not known.

The Young's moduli in the direction perpendicular to the chain axis of the PVA crystal are appreciably larger and the linear compressibilities are smaller than those of the PE crystal as shown below, reflecting the strength of hydrogen bonding forces.

	Young's modulus, $\times 10^{10}$ dyn/cm ²	linear compressibility, $\times 10^{-12}$ cm ² /dyn
PVA	22.0-8.5	1.9-7.7
PE	9.2-6.9	6.8-9.7

On the other hand, the value of Young's modulus (287.4×10^{10} dyn/cm²) in the chain direction of PVA is in the same order as that of PE (315.5×10^{10} dyn/cm²), which is in the range characteristic to the planar-zigzag chain. This may suggest that the intermolecular interactions (even for appreciably strong hydrogen bonding) hardly affect the Young's modulus in the chain direction, which is mainly determined by the strong covalent bondings and conformation of the skeletal chain. In fact, the calculated value of Young's modulus along the chain direction without taking into account the intermolecular hydrogen bondings is 287.2×10^{10} dyn/cm², almost the same as the value considering the hydrogen bonds. These circumstances can be shown also for the cases of other polymers such as poly(vinylidene fluoride), whose mechanical properties are governed by the electrostatic interactions. The calculated results for crystallite moduli of poly(vinylidene fluoride)

will be reported in a subsequent paper.²²

References and Notes

- (1) K. Tashiro, M. Kobayashi, and H. Tadokoro, *Macromolecules*, preceding paper in this issue.
- (2) I. Sakurada and K. Kaji, *J. Polym. Sci., Part C*, **31**, 57 (1970); K. Kaji, Doctoral Thesis, Kyoto University, 1970.
- (3) T. Ito, *J. Soc. Fiber Sci. Technol. Jpn.*, **32**, P-46 (1976).
- (4) M. Born and K. Huang, "Dynamical Theory of Crystal Lattices", Oxford University Press, London, 1954.
- (5) A. Odajima and T. Maeda, *J. Polym. Sci., Part C*, **15**, 55 (1966).
- (6) G. Wobser and S. Blasenbrey, *Kolloid Z. Z. Polym.*, **241**, 985 (1970).
- (7) T. Kitagawa and T. Miyazawa, *Adv. Polym. Sci.*, **9**, 335 (1972).
- (8) M. Kobayashi and H. Tadokoro, *J. Chem. Phys.*, **66**, 1258 (1977).
- (9) Y. Ueda, Y. Chatani, and H. Tadokoro, *Polym. Prepr., Jpn.*, **26**, 1326 (1977).
- (10) C. W. Bunn, *Nature (London)*, **161**, 929 (1948).
- (11) I. Nitta, I. Taguchi, and Y. Chatani, *Annu. Rept. Inst. Textile Sci. Jpn.*, **10**, 1 (1957).
- (12) T. Ito and S. Fujita, *Polym. Prepr., Jpn.*, **27**, 531 (1978).
- (13) J. F. Nye, "Physical Properties of Crystals", Oxford at the Clarendon Press, Oxford, 1957.
- (14) R. F. Schaufele and T. Shimanouchi, *J. Chem. Phys.*, **47**, 3605 (1967).
- (15) G. R. Strobl and R. Eckel, *J. Polym. Sci., Polym. Phys. Ed.*, **14**, 913 (1976).
- (16) L. Holliday and J. W. White, *Pure Appl. Chem.*, **26**, 545 (1971).
- (17) R. F. S. Hearmon, *Rev. Mod. Phys.*, **18**, 409 (1946); *Adv. Phys.*, **5**, 323 (1956).
- (18) K. Tashiro, M. Kobayashi, and H. Tadokoro, *Macromolecules*, **10**, 413 (1977).
- (19) K. Tashiro, M. Kobayashi, and H. Tadokoro, *Macromolecules*, **10**, 731 (1977).
- (20) M. Hikosaka, S. Minomura, and T. Seto, *Polym. Prepr. Jpn.*, **25**, 945 (1976).
- (21) K. Tashiro, M. Kobayashi, and H. Tadokoro, *Polym. Bull.*, in press.
- (22) K. Tashiro, M. Kobayashi, and H. Tadokoro, to be published.
- (23) G. T. Davis, R. K. Eby, and J. P. Colson, *J. Appl. Phys.*, **41**, 4316 (1970).
- (24) M. Tasumi and T. Shimanouchi, *J. Chem. Phys.*, **43**, 1245 (1965).

Use of a Gas Chromatographic Technique for the Study of the Variation of the Interaction Energy Parameter with Temperature

P. J. T. Tait* and A. M. Abushihada

Department of Chemistry, U.M.I.S.T., Manchester, England.

Received October 25, 1977

ABSTRACT: The dependence of the interaction energy parameter is investigated by means of a gas-liquid chromatographic technique for the solutes tetrahydrofuran, methyl ethyl ketone, diethyl ketone, ethyl propyl ketone, and toluene in poly(vinyl chloride), polystyrene, and poly(methyl methacrylate) used as stationary phases. In all cases plots of the interaction energy parameter against temperature showed positive minima and curvature which remained positive throughout the range of temperature which was investigated in agreement with more recent theoretical predictions. The results obtained are discussed in terms of concepts of contact energy dissimilarity and free volume dissimilarity between the solute and polymer molecules.

The use of a polymeric stationary phase in gas-liquid chromatographic studies of polymer-solute interactions was first made in 1969 by Smidsrød and Guillet¹ who determined values for the activity coefficients of various solutes such as acetic acid, butyl alcohol, α -chloronaphthalene, naphthalene, and hexadecane at near infinite dilution (near zero solute concentration) in a poly(*N*-isopropylacrylamide) stationary phase. Since this initial application gas-liquid chromatography, GLC, has been used by a number of investigators²⁻¹⁵ to obtain infinite dilution data on a number of polymeric systems, since under these experimental conditions one is effectively studying the properties of solvent molecules isolated in pure polymer. Both polar^{1,8,14,15} and nonpolar^{4-7,11,14,15}

solutes have been used over a fairly wide range of temperature (25-100 °C).

In an earlier publication¹⁶ we have established that values of χ_1 , obtained from GLC measurements, are in close agreement with those determined using the vapor pressure method. In the present study the dependence of the interaction parameter, χ_1 , on temperature is investigated for tetrahydrofuran, methyl ethyl ketone, diethyl ketone, ethyl propyl ketone, and toluene at infinite dilution in the stationary polymeric phases poly(vinyl chloride), polystyrene, and poly(methyl methacrylate). These results are considered to be of relevance in that they demonstrate the usefulness of GLC in providing information concerning polymer solute interactions and their variation with